inventions

Article

Integral Equations of the First Kind for Calculating Electro- and Magnetostatic Fields Perturbed by Conductors and Ferro-Magnets

Yurij Plugatar [1], Dmitriy Filippov [2], Vladimir Chabanov [2], Anatoliy Kazak [3,*], Vadim Korzin [1], Nikolay Oleinikov [3], Angela Mayorova [3] and Dmitry Nekhaychuk [4]

[1] Nikitsky Botanical Gardens—National Scientific Center of Russian Academy of Sciences, 298648 Yalta, Russia
[2] Institute of Physics and Technology, V.I., Vernadsky Crimean Federal University, 295007 Simferopol, Russia
[3] Humanitarian Pedagogical Academy, V.I. Vernadsky Crimean Federal University, 295007 Simferopol, Russia
[4] Plekhanov Russian University of Economics, 115093 Moscow, Russia
* Correspondence: kazak@cfuv.ru or kazak_a@mail.ru

Abstract: The aim of the study was to develop a methodology for calculating and optimizing devices for the magnetic exploration of fossils containing materials with a high magnetic permeability. The proposed technique is based on the calculation of electrostatic fields perturbed by conducting bodies and of magnetic fields perturbed by ferromagnets with a high magnetic permeability. It uses an integral equation of the first kind. This technique is preferable to the technique consisting in the use of an integral equation of the second kind, since in the situation under consideration, the latter does not have a unique solution and requires transformation. Prospects for the development of this area allow one to bring geophysical services to the service market on a new scientific and technical production level; reduce the environmental burden on nature by replacing magnetometric measurements with energy-saving, environmentally safe technology; and ensure the export potential of magnetometric equipment.

Keywords: permanent magnet; conductor; ferromagnet; magnetic field; electric field; integral equation; system of linear algebraic equations; magnetization; electric field strength; magnetic field strength; magnetic field induction

check for updates

Citation: Plugatar, Y.; Filippov, D.; Chabanov, V.; Kazak, A.; Korzin, V.; Oleinikov, N.; Mayorova, A.; Nekhaychuk, D. Integral Equations of the First Kind for Calculating Electro- and Magnetostatic Fields Perturbed by Conductors and Ferro-Magnets. *Inventions* **2023**, *8*, 55. https://doi.org/10.3390/inventions8020055

Academic Editors: Alessandro Chiolerio and M. M. Bhatti

Received: 2 December 2022
Revised: 29 January 2023
Accepted: 7 March 2023
Published: 10 March 2023

1. Introduction

The aim of the study was to develop a methodology for calculating and optimizing devices for the magnetic exploration of fossils containing materials with a high magnetic permeability.

Magnetic prospecting is based on the differentiation of rocks and ores according to their physical properties. The main magnetic characteristics of any medium are magnetic susceptibility and magnetization. Magnetic susceptibility is characterized by the ability of minerals and rocks to be magnetized under the action of an external magnetic field, and magnetization is the magnetic moment per unit volume of the rock. The magnetic properties of minerals are determined by the chemical composition and structure of the crystal lattice, and the magnetic properties of rocks depend on their mineral composition, texture and structure, temperature, and pressure [1–3].

A modern magnetic-prospecting measuring device consists of a number of mandatory components: a sensor, an amplifier, a signal meter, and an analog-to-digital converter (ADC). However, the most important component is still the sensor. The sensor is a primary converter, an element of a measuring, signaling, regulating or controlling device of a system that converts a controlled value (pressure, temperature, frequency, speed, displacement, voltage, electric current, etc.) into a signal that is convenient for measurement, transmission, conversion, storage, and registration, as well as for their impact on managed processes [4–6].

Magnetometers differ in their principle of operation from magnetically sensitive sensors, which determine which field components the magnetometer is able to measure. The classification of magnetometers according to the principle of operation is given in Table 1. T is the total vector of the Earth's magnetic field (EMF), and the physical essence of T is magnetic induction, where Z is the vertical component of the total EMF vector, H is its horizontal component, X is its northern component, and Y is its eastern component. In a physical meaning, each of these components is an induction [7–11]. Devices with a different principle of operation have certain advantages and shortcomings.

Table 1. Classification of magnetometers according to the principle of operation.

Magnetometer Type	Magnetic Sensitive Element	Measured Components
Optical-mechanical	Permanent magnet	Z, ΔZ
Proton	Hydrogen liquid	
Overhauser	Hydrogen-containing liquid with the addition of free radicals with unpaired electrons	T, ΔT, ∂T ∂x, ∂T ∂x
Quantum	Alkali metal vapors	
Ferroprobe	Ferrosonde	X, Y, Z, ΔX, ΔY, ΔZ
Cryogenic	Superconducting quantum interferometer	T, ΔT

A magnetic-field sensitivity G is one of the crucial parameters of the magnetometer. At the same time, it is almost impossible to formalize this parameter, to make it the same for all magnetometers, and this is not only the case because magnetometers differ in their principle of operation but also because they do so in the design of the transducers and the signal-processing function. For magnetometers, sensitivity to a magnetic field is usually denoted by the value of the magnetic-field induction, which the device is able to register. Usually, the sensitivity G is measured in nanotesla.

The main positive and negative qualities of different types of magnetometers are given in the Table 2.

Table 2. Comparative characteristics of various types of magnetometers.

Magnetometer Type	Advantages	Disadvantages
Optical-mechanical	Able to measure Z, X, Y and H components.	Zero point creep, presence of azimuth correction, temperature drift, low measurement speed, low accuracy.
Proton	This magnetometer type is impervious to shaking and vibrations, measurements are practically independent of changes in external conditions (temperature, humidity, pressure), there is no need for precise orientation of the sensor, there is no need to stake out reference networks, zero-point shift is negligible.	Instability and signal loss at high magnetic field gradients.
Overhauser	All the benefits of proton magnetometers, plus reduced measurement time, lower uncertainty due to increased signal-to-noise ratio, small sensor size.	Short lifetime of the working substance, the appearance of a systematic error, due to the influence of the microwave unit.
Quantum	High measurement speed, high resolution.	The need for orientation of the sensor is present, but with small values: orientation and azimuth errors, temperature drift. Sensitivity to mechanical influences (shock, vibration).
Ferroprobe	Able to measure Z, X, Y and H components with high accuracy.	The bulkiness of the equipment, the need to orient the sensor.
Cryogenic	High accuracy.	The need to maintain very low temperatures for a superconductor. There are no mass-produced devices.

The processing of magnetic survey data is aimed at eliminating various kinds of "interference" from the primary data, for example, variations, the normal gradient of the Earth's magnetic field, and others [12–15]. The result of processing should be maps and maps of graphs of the anomalous magnetic field (Figure 1).

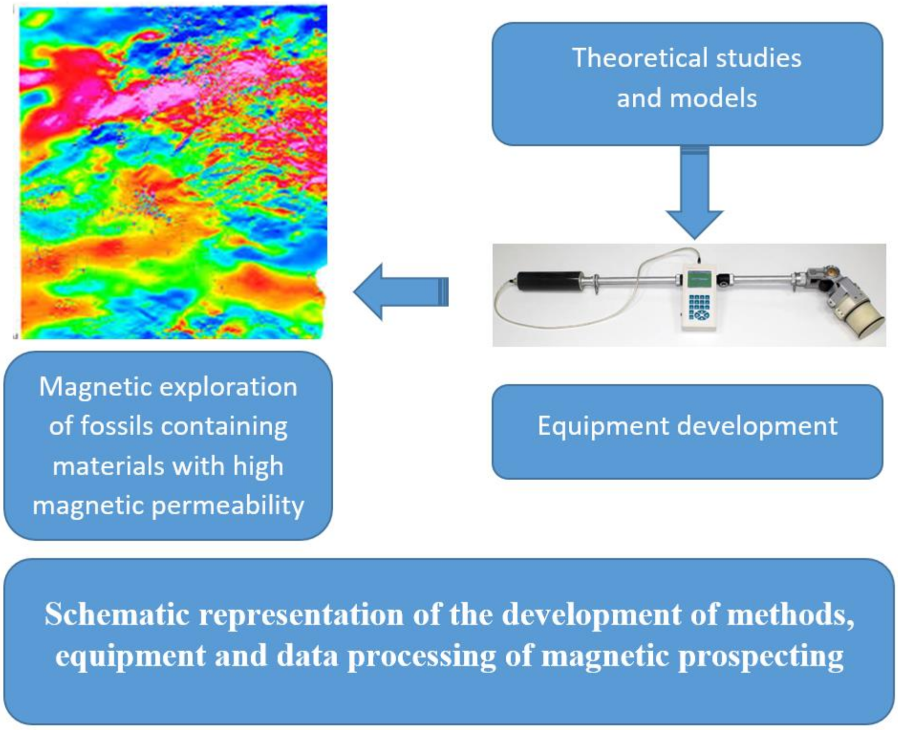

Figure 1. Schematic representation of the development of methods, equipment, and data processing of magnetic prospecting.

The goal of this research was to develop a method for the magnetic prospecting of, predominantly, fossils containing materials with a high magnetic permeability.

Materials with a high magnetic permeability exist; for example, permalloys belong to them. Pure iron also has a fairly high magnetic permeability. The infinite magnetic permeability of a material is, of course, a mathematical abstraction. However, in the absence of the phenomenon of magnetic saturation in a ferromagnet under certain conditions of the problem, if the magnetic permeability of the material of this ferromagnet is sufficiently large and is, for example, 1000 μ_0 or higher, then the field perturbed by such a material will practically not differ in any way from the field perturbed by a ferromagnet with an infinite magnetic permeability [16–19].

Problems of electrostatics and magnetostatics are considered and solved. The basic integral equations of electro-magnetostatics are reduced to linear algebraic equations, which, in particular, can be solved using a numeric computing environment. The equations for magnetic charges are similar to the equations for electric charges, so they have the same form in this approximation. Since a system of linear equations of a sufficiently large order is used to solve integral equations, it is advisable to use a numeric computing environment to solve them [20–23].

In the introduction of this study, we have tried to provide:

- a brief overview of the comparative characteristics of various types of magnetometers;
- a schematic representation of the development of methods, equipment, and data processing of magnetic prospecting;
- the goal of this research as the development of a method for magnetic prospecting of, predominantly, fossils containing materials with a high magnetic permeability.

In this study, the following options are considered (Figure 2):

(A) Electrostatic fields. Three-dimensional case, where a conducting body bounded by a closed surface S carrying a charge q is introduced into the field of charges located in volume V_0.

(B) The field of a permanent magnet. Three-dimensional case, where a magnetic system consists of a permanent magnet with a given distribution of the magnetization vector

(V_0 is the volume occupied by the magnet) and a homogeneous ferromagnet bounded by a closed surface S.

(C) Electrostatic field. The plane-parallel case, where the system is extended along the z axis.

(D) The field of a permanent magnet. Plane-parallel case, where the magnetic system is extended along the z axis.

Figure 2. Options considered in this study.

Electrostatic fields. Three-dimensional case. Let a conducting body bounded by a closed surface S carrying a charge q be introduced into the field of charges located in volume V_0 (Figure 3) [24–26].

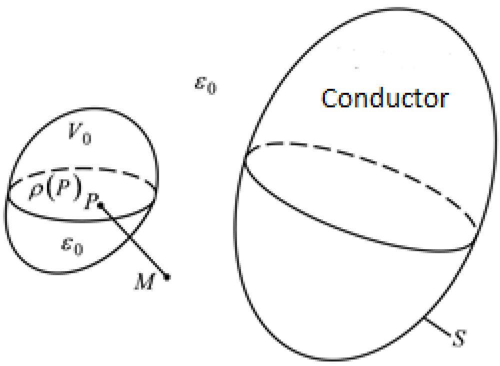

Figure 3. A conducting body bounded by a closed surface S carrying a charge q is introduced into the field of charges located in volume V_0.

It is required that one find the electric field $\vec{E}$ outside S (inside S field $\vec{E} = 0$).

Take the point of the zero value of the potential at infinity. Then, for the potential at any point M, we can write the expression:

$$\varphi(M) = \frac{1}{4\pi\varepsilon_0}\int\limits_{V_0} \frac{\rho(P)}{r_{PM}}dV_P + \frac{1}{4\pi\varepsilon_0}\oint\limits_{S} \frac{\sigma(P)}{r_{PM}}dS_P \tag{1}$$

where $\rho(P)$ is a given distribution of the electric-charge density in a closed volume V_0, and $\sigma(P)$ is an unknown distribution of the surface-electric-charge density on a given surface S.

Using the expression for the potential at an arbitrary point Q (1) on the surface S and equating it with the as yet unknown constant C, we obtain an integral equation of the first kind for $\sigma(P)$:

$$\frac{1}{4\pi\varepsilon_0}\oint\limits_{S} \frac{\sigma(P)}{r_{PQ}}dS_P = C + f(Q),\ \frac{\sigma(P)}{r_{PQ}}. \tag{2}$$

where:

$$f(Q) = -\frac{1}{4\pi\varepsilon_0}\int\limits_{V_0} \frac{\rho(P)}{r_{PQ}}dV_P$$

The unknowns in Equation (2) are $\sigma(P)$ and C.

When deriving integral Equation (2), information about the total charge of the conductor was not used. Therefore, this equation will have a non-unique solution.

In fact, if we fix $C = C'$, then from (2), we can find $\sigma'(P)$. This distribution satisfies the equation:

$$\frac{1}{4\pi\varepsilon_0}\oint\limits_{S} \frac{\sigma'(P)}{r_{PQ}}dS_P = C' + f(Q),\ Q \in S. \tag{3}$$

If fixed $C = C'' \neq C'$, then Equation (2) will have a solution:

$$\frac{1}{4\pi\varepsilon_0}\oint\limits_{S} \frac{\sigma''(P)}{r_{PQ}}dS_P = C'' + f(Q),\ Q \in S. \tag{4}$$

The solution $\{\sigma''(P),\ C''\}$ differs from the solution $\{\sigma'(P),\ C'\}$, at least because $C'' \neq C'$. It is easy to see that $\sigma''(P)$ is not identically equal to $\sigma'(P)$, since if we assume that $\sigma''(P) \equiv \sigma'(P)$, then subtracting the expression (4) from (3), we obtain:

$$0 = C' - C'' + 0.$$

This contradiction definitively proves that the solution of integral Equation (2) is not unique.

To (2) we must add the equation:

$$\oint\limits_{S} \sigma(P)dS_P = q \tag{5}$$

2. Materials and Methods

The system of integral Equations (2) and (5) has a unique solution.

Assuming two different solutions of the system (2) and (5) $\{\sigma'(P),\ C'\}$ and $\{\sigma''(P),\ C''\}$, for the difference distribution $\{\sigma'''(P),\ C'''\} = \{\sigma'(P) - \sigma''(P),\ C' - C''\}$, we obtain the equations:

$$\frac{1}{4\pi\varepsilon_0}\oint\limits_{S} \frac{\sigma'''(P)}{r_{PQ}}dS_P = C''', Q \in S. \tag{6}$$

$$\oint\limits_{S} \sigma'''(P)dS_P = 0 \tag{7}$$

The system of integral Equations (6) and (7) describes the distribution of the surface-charge density on a solitary uncharged conductor. Such a distribution is obviously $\sigma'''(P) \equiv 0$. But then, as follows from (6), $C''' = 0$. Thus, the uniqueness of the solution of the system of integral Equations (2) and (5) is proven [21–32].

The system of Equations (2) and (5) can be solved by reducing it to a system of linear algebraic equations. We divide the surface S into N elementary surfaces ΔS_i (i = 1, 2 . . . N). On each such surface ΔS_i, the surface σ density will be σ_i, considered constant and equal. Then, instead of (2), we can write:

$$\frac{1}{4\pi\varepsilon_0}\sum_{i=1}^{N}\sigma_i\int\limits_{\Delta S_i}\frac{dS_P}{r_{PQ}} - C = f(Q), Q \in S, \tag{8}$$

and instead of (5):

$$\sum_{i=1}^{N}\sigma_i \cdot \Delta S_i = q \tag{9}$$

Let us take the point Q_k approximately in the center of the site ΔS_k; if $i \neq k$, then approximately replace the integrals in (8) with the value:

$$\int\limits_{\Delta S_i}\frac{dS_P}{r_{PQ}} = \frac{\Delta S_i}{r_{P_iQ_k}} \tag{10}$$

Then, instead of (8), we obtain the equations:

$$\frac{1}{4\pi\varepsilon_0}\sum_{\substack{i=1\\ i\neq k}}^{N}\frac{\sigma_i\Delta S_i}{r_{P_iQ_k}} + \frac{1}{4\pi\varepsilon_0}\sigma_k\int\limits_{\Delta S_k}\frac{dS_P}{r_{PQ_k}} - C = f(Q_k), k = 1, 2, \ldots, N. \tag{11}$$

Equations (9) and (11) are a system of linear algebraic equations consisting (SLAE) of N + 1 equations with N + 1 unknowns: $\sigma_1, \sigma_2, \ldots, \sigma_N, C$.

The integral included in (11) can be taken analytically. For example, for the case when ΔS_k, there is a rectangle with sides 2a and 2b, and the point Q_k is in the center of the rectangle; this integral is equal to (calculations are omitted):

$$\int\limits_{\Delta S_k}\frac{dS_P}{r_{PQ_k}} = 4\left(a\ln tg\left(0.25\pi + 0.5arctg\frac{b}{a}\right) - b\ln tg\left(0.5arctg\frac{b}{a}\right)\right) \tag{12}$$

Or:

$$\int\limits_{\Delta S_k}\frac{dS_P}{r_{PQ_k}} = 4(a\ln(b+l) + b\ln(a+l) - a\ln a - b\ln b) \tag{13}$$

where: $l = \sqrt{a^2 + b^2}$.

3. Results and Discussion

Let us consider the second way of solving the system of integral Equations (2) and (5). We find the solution of the equation:

$$\frac{1}{4\pi\varepsilon_0}\oint\limits_{S}\frac{\sigma_1(P)}{r_{PQ}}dS_P = f(Q),\ Q \in S. \tag{14}$$

This solution $\sigma_1(P)$ can be found by reducing integral Equation (14) to a SLAE with a matrix $N \times N$.

Next, we find the solution of the equation:

$$\frac{1}{4\pi\varepsilon_0}\oint_S \frac{\sigma_1(P)}{r_{PQ}}dS_P = 1,\ Q \in S. \tag{15}$$

Obviously, the solution of the system (2) and (5) will be equal to:

$$\sigma(P) = \sigma_1(P) + C\cdot\sigma_2(P) \tag{16}$$

where:

$$C = \frac{q - q_1}{q_2} \tag{17}$$

$$q_1 = \oint_S \sigma_1(P)dS_P,\ q_2 = \oint_S \sigma_2(P)dS_P. \tag{18}$$

A special case of the considered problem is the case when there is no external electric field, and the conductor carries a charge q, i.e., these are the problems for finding the charge-density distribution on a solitary charged conductor. These problems are described by integral equations:

$$\frac{1}{4\pi\varepsilon_0}\oint_S \frac{\sigma(P)}{r_{PQ}}dS_P = C, \tag{19}$$

$$\oint_S \sigma(P)dS_P = q. \tag{20}$$

The first way to solve this system is the same as for the system (2) and (5).

The second way for the system (19) and (20) will look like this. We fix the constant $C = C_1$. We find the solution of the equation:

$$\frac{1}{4\pi\varepsilon_0}\oint_S \frac{\sigma_1(P)}{r_{PQ}}dS_P = C_1. \tag{21}$$

We reduce, as before, to SLAE.

We find:

$$q_1 = \oint_S \sigma_1(P)dS_P. \tag{22}$$

The desired solution will obviously be equal to:

$$C = \frac{q}{q_1}C_1, \sigma(P) = \frac{q}{q_1}\sigma_1(P). \tag{23}$$

After finding the distribution $\sigma(P)$, the electric field strength at any point M can be found by the formula:

$$\vec{E}(M) = \frac{1}{4\pi\varepsilon_0}\int_{V_0} \frac{\rho(P)\ \vec{r}_{PM}}{r_{PM}^3}dV_P + \frac{1}{4\pi\varepsilon_0}\oint_S \frac{\sigma(P)\ \vec{r}_{PM}}{r_{PM}^3}dS_P. \tag{24}$$

3.1. The Field of a Permanent Magnet—Three-Dimensional Case

Consider a magnetic system consisting of a permanent magnet with a given distribution of the magnetization vector $\vec{M}(P)$ ($P \in V_0$, V_0 is the volume occupied by the magnet) and a homogeneous ferromagnet bounded by a closed surface S (Figure 4).

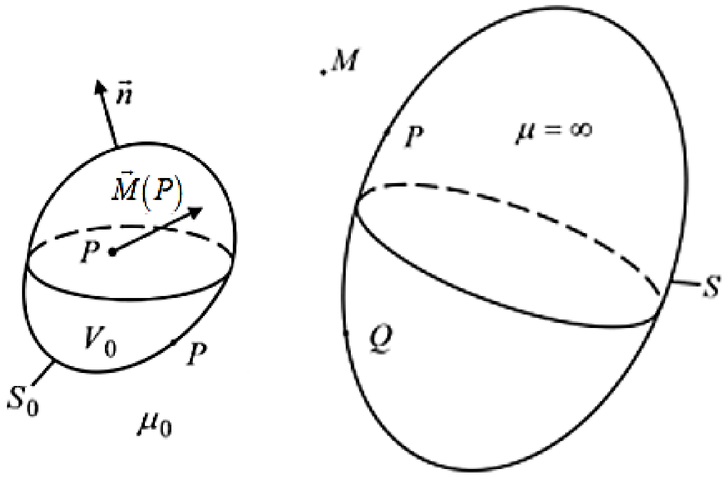

Figure 4. A magnetic system consisting of a permanent magnet with a given distribution of the magnetization vector $\vec{M}(P)$ ($P \in V_0$, V_0 is the volume occupied by the magnet) and a homogeneous ferromagnet bounded by a closed surface S.

The magnetic permeability of a ferromagnet will be considered constant and equal to infinity. The magnetic permeability of the medium surrounding the magnet and ferromagnet is equal to μ_0.

The geometric parameters of the system are assumed to be set.

To calculate the magnetic field, this system can be replaced with magnetic charges located in the air. By definition, the magnetic charge density ρ is called:

$$\rho = div\, \vec{H}, \tag{25}$$

where $\vec{H}$ is the magnetic field strength.

Since $\vec{H} = \frac{\vec{B}}{\mu_0} - \vec{M}$, where $\vec{B}$ is the magnetic field induction, from (20) we then obtain:

$$\rho = -div\, \vec{M}, \tag{26}$$

Because: $div\vec{B} = 0$.

From (21), we find that there are also magnetic charges with a surface density on the surface of the magnet $S_{0:}$

$$\sigma_0 = M_n, \tag{27}$$

where M_n is the normal component of the vector $\vec{M}$ on the surface of the magnet S_0 (the direction of the normal is chosen on the exterior of the magnet).

Surface magnetic charges also exist on the surface S of a ferromagnet. Inside a ferromagnet at $\mu = const$, the bulk density of magnetic charges is:

$$\rho = div\, \vec{H} = div\, \frac{\vec{B}}{\mu} = \frac{1}{\mu} div\, \vec{B} = 0.$$

For the case when $\mu = \infty$, $\vec{H} = 0$ inside a ferromagnet, and therefore:

$$\rho = div\, \vec{H} = 0.$$

We introduce the scalar magnetic potential φ by equality:

$$-\, grad\varphi = \vec{H} \tag{28}$$

or:

$$\varphi(M) = \int_{M}^{M_0} \vec{H} d\vec{l} \tag{29}$$

where M_0 is the point of the zero value of the potential.

By analogy with electrostatics:

$$\varphi(M) = \frac{1}{4\pi} \int_{V_0} \frac{\rho(P)}{r_{PM}} dV_P + \frac{1}{4\pi} \oint_{S_0} \frac{\sigma_0(P)}{r_{PM}} dS_P + \frac{1}{4\pi} \oint_{S} \frac{\sigma(P)}{r_{PM}} dS_P, \tag{30}$$

where M is an arbitrary point of space.

Since inside the ferromagnet $\vec{H} = 0$, the surface S is equipotential. Having recorded this fact mathematically, we obtain an integral equation of the first kind for σ:

$$\frac{1}{4\pi} \oint_{S} \frac{\sigma(P)}{r_{PQ}} dS_P - C = -\frac{1}{4\pi} \int_{V_0} \frac{\rho(P)}{r_{PQ}} dV_P - \frac{1}{4\pi} \oint_{S_0} \frac{\sigma_0(P)}{r_{PQ}} dS_P,\ Q \in S \tag{31}$$

where C is an unknown constant.

Denoting the right part (26) by $f(Q)$, we finally obtain the following integral equation of the first kind:

$$\frac{1}{4\pi} \oint_{S} \frac{\sigma(P)}{r_{PQ}} dS_P = C + f(Q). \tag{32}$$

This is an analogue of Equation (2) in electrostatics.

To derive an equation that is an analogue of Equation (5), we do the following.

Let us take a closed surface S' located in the air and close to the surface S, i.e., only a ferromagnet is located inside the closed surface. For this surface, one can write:

$$\oint_{S'} \vec{H} d\vec{S} = \frac{1}{\mu_0} \oint_{S'} \vec{B} d\vec{S} - \oint_{S'} \vec{M} d\vec{S} = \frac{1}{\mu_0} \cdot 0 - 0 = 0 \tag{33}$$

However, as follows from (25) and from the fact that there are no magnetic charges in the ferromagnet volume:

$$\oint_{S'} \vec{H} d\vec{S} = \oint_{S} \sigma\, dS \tag{34}$$

From (33) and (34), the integral equation follows, which is an analogue of Equation (5):

$$\oint_{S} \sigma\, dS = 0 \tag{35}$$

The system of integral Equations (32) and (35) can be solved along with the system (2, 5) in two ways. In this case, $q = 0$ is assumed.

A special case when there is no external magnetic field for magnetostatics does not exist, because for magnetostatics $\oint_{S} \sigma dS = 0$ always applies, and therefore, if there is no external magnetic field, then $\sigma \equiv 0$.

After finding the distribution $\sigma(P)$ of the field of tension, $\vec{H}(M)$ can be found by the formula:

$$\vec{H}(M) = \frac{1}{4\pi} \int_{V_0} \frac{\rho(P)\ \vec{r}_{PM}}{r_{PM}^3} dV_P + \frac{1}{4\pi} \oint_{S_0} \frac{\sigma_0(P)\ \vec{r}_{PM}}{r_{PM}^3} dS_P + \frac{1}{4\pi} \oint_{S} \frac{\sigma(P)\ \vec{r}_{PM}}{r_{PM}^3} dS_P.$$

Additionally, we find the induction of the magnetic field $\vec{B}(M)$ according to the formula:

$$\vec{B}(M) = \mu_0 \vec{H}(M) + \mu_0 \vec{M}(M)$$

The latter formula allows us to find $\vec{B}(M)$ at all points outside the ferromagnet. We do not consider the question of finding $\vec{B}(M)$ inside a ferromagnet here.

3.2. The Electrostatic Field—The Plane-Parallel Case

In the case of an extended system along the z axis (Figure 5), the corresponding integral equations will have the form:

$$\frac{1}{2\pi\varepsilon_0} \oint_l \sigma(P) \ln \frac{1}{r_{PQ}} dl_P = C + f(Q),\ Q \in l, \tag{36}$$

$$\oint_l \sigma(P) dl_P = \tau, \tag{37}$$

$$f(Q) = -\frac{1}{2\pi\varepsilon_0} \int_{S_0} \rho(P) \ln \frac{1}{r_{PQ}} dS_P,$$

τ—a given total charge of the conductor per unit length along z.

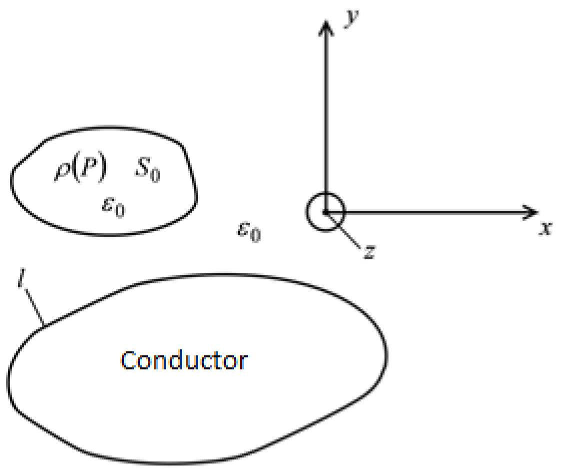

Figure 5. Electrostatic field, plane-parallel case, assuming an extended system along the z-axis.

When solving the system (36) and (37), the line l will be divided into N elementary lines, on each of which the surface density σ will be assumed to be constant. In this case, we will need to analytically calculate the integral of the form:

$$\int_{\Delta l_k} dl_P \ln \frac{1}{r_{PQ}}.$$

If Δl_k is a straight-line segment and the point Q is located in the center of the segment, then:

$$\int_{\Delta l_k} dl_P \ln \frac{1}{r_{PQ}} = 2(a - a \ln a). \tag{38}$$

where a is half the length of the segment.

After finding $\sigma(P)$, the tension $\vec{E}(M)$ can be found by the formula:

$$\vec{E}(M) = \frac{1}{2\pi\varepsilon_0}\int\limits_{S_0} \frac{\rho(P)\ \vec{r}_{PM}}{r_{PM}^2} dS_P + \frac{1}{2\pi\varepsilon_0}\oint\limits_{l} \frac{\sigma(P)\ \vec{r}_{PM}}{r_{PM}^2} dl_P.$$

Along with the electrostatic three-dimensional case, a special case of the considered problem is possible when it is necessary to find the field of a solitary charged conductor. This case is described by the equations:

$$\frac{1}{2\pi\varepsilon_0}\oint\limits_{l} \sigma(P) \ln\frac{1}{r_{PQ}} dl_P = C, Q \in l,$$

$$\oint\limits_{l} \sigma(P) dl_P = \tau,$$

whose solution is similar to the three-dimensional case.

3.3. The Field of a Permanent Magnet—The Plane-Parallel Case

In the case of an extended magnetic system along the z axis (Figure 6), the corresponding integral equations will have the form:

$$\frac{1}{2\pi}\oint\limits_{l} \sigma(P) \ln\frac{1}{r_{PM}} dl_P = C + f(Q),\ Q \in l, \tag{39}$$

$$\oint\limits_{l} \sigma(P) dl_P = 0 \tag{40}$$

$$f(Q) = -\frac{1}{2\pi}\int\limits_{S_0} \rho(P) \ln\frac{1}{r_{PM}} dS_P - \frac{1}{2\pi}\oint\limits_{l_0} \sigma_0(P) \ln\frac{1}{r_{PM}} dl_P$$

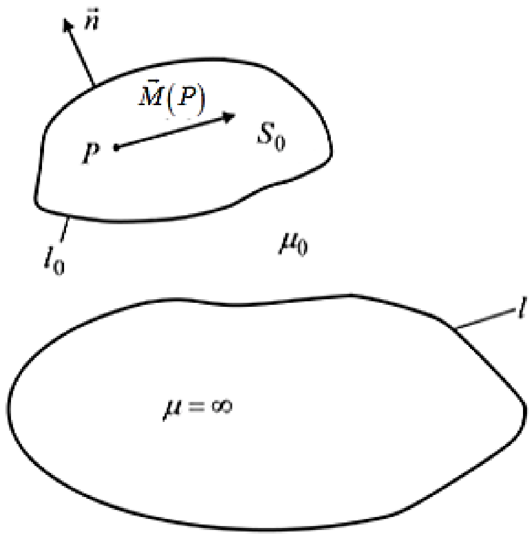

Figure 6. Field of a permanent magnet, plane-parallel case, under the condition of a magnetic system extended along the z axis.

These equations are solved by analogy with the equations of electrostatics (31, 32), in which it is necessary to accept $\tau = 0$. After finding the distribution σ, the tension $\vec{H}(M)$ and induction $\vec{B}(M)$ are calculated using the formulas:

$$\vec{H}(M) = \frac{1}{2\pi}\int_{S_0} \frac{\rho(P)\,\vec{r}_{PM}}{r_{PM}^2} dS_P + \frac{1}{2\pi}\oint_{l_0} \frac{\sigma_0(P)\,\vec{r}_{PM}}{r_{PM}^2} dl_P + \frac{1}{2\pi}\oint_{l} \frac{\sigma(P)\,\vec{r}_{PM}}{r_{PM}^2} dl_P.$$

$$\vec{B}(M) = \mu_0 \vec{H}(M) + \mu_0 \vec{M}(M)$$

3.4. Examples of Calculating Magnetic Fields Using Integral Equations of the First Kind

The magnetic field of the system shown in Figure 7 was calculated. The permanent magnet and ferromagnets have the shape of a parallelepiped. The centers of these parallelepipeds lie on the y axis. The magnet is magnetized uniformly along the y-axis, i.e., $\vec{M} = M\vec{e}_y$. Therefore, $\rho = 0$ in the volume of the magnet.

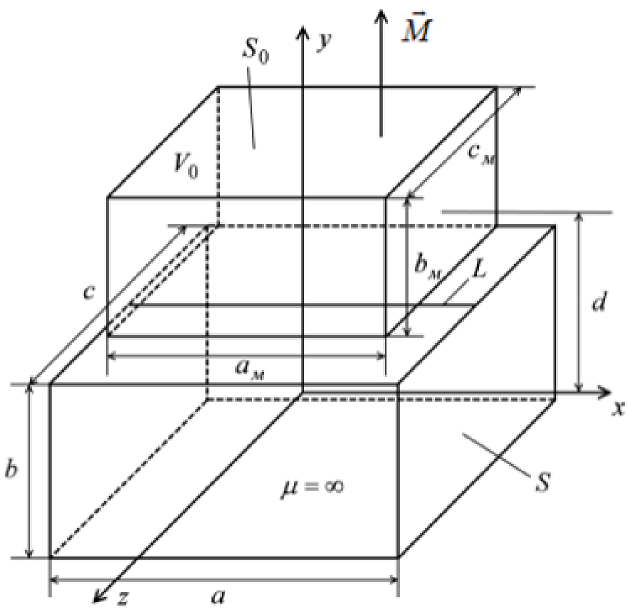

Figure 7. The magnetic field of the system for which the calculation was made using integral equations of the first kind.

After calculating the distribution σ, the potential on the segment L of the upper face of the ferromagnet was calculated. The results are presented in Table 3, with the numbering of points from left to right. The magnetic-field induction was also calculated at the center of the magnet B_1 = 1.749 Tl (the first method), B_1 = 1.749 Tl (the second method) and at a point on the y axis at a distance of 0.0025 m from the ferromagnet, i.e., at the point y = 0.0275 m. It was equal to B_2 = 0.644 Tl (the first method) and B_2 = 0.644 Tl (the second method). At the same point, the induction was calculated in the absence of a ferromagnet. It was equal to B'_2 = 0.365 Tl.

A plane-parallel version of this system was also calculated, i.e., when $c = \infty$, $c_{\mathcal{M}} = \infty$, and N was taken to be 256. The value of the potential on line L is shown in Table 4. B_1 = 1.817 Tl (first method), B_1 = 1.817 Tl (second method), B_2 = 0.44 Tl (first method), and B_2 = 0.444 Tl (second method). B'_2 = 0.268 Tl.

Table 3. Calculation of the potential on the segment L of the upper face of the ferromagnet after calculating the distribution σ.

The First Way	The Second Way
−2410.29	−2410.29
−2368.50	−2368.50
−2354.42	−2354.42
−2353.95	−2353.95
−2354.71	−2354.71
−2354.71	−2354.71
−2353.95	−2353.95
−2354.42	−2354.42
−2368.50	−2368.50
−2410.29	−2410.29

Table 4. Calculation of the potential on the line L in the case of a plane-parallel version of this system, when $c = \infty$ and $c_{\mathcal{M}} = \infty$. N was taken to be 256.

The First Way	The Second Way
−6020.20	−6020.20
−6008.95	−6008.95
−6004.63	−6004.63
−6004.21	−6004.21
−6004.25	−6004.25
−6004.25	−6004.25
−6004.21	−6004.21
−6004.63	−6004.63
−6008.95	−6008.95
−6020.20	−6020.20

4. Conclusions

Modifications of this calculation method were also used by the authors when modeling the winding of electric motors (for pumps, cars, tractors, drones), generators, permanent-magnet linear motors for machine tools, etc.

Two solutions are proposed for the obtained integral equations of the first kind. Both methods, as shown by examples of calculating magnetic fields created by permanent magnets and perturbed by ferromagnets with a magnetic permeability $\mu = \infty$, give the same results. Numerical examples also show that the SLAE to which the integral equation of the first kind is reduced is easily solved.

The existing methods of magnetic prospecting have both advantages and disadvantages. The development of new methods can open up new possibilities, increase the accuracy of calculations, increase the efficiency and reliability of equipment, and help reduce the cost of equipment and research in the field of magnetic prospecting. The proposed methods can be applied to the calculation and optimization of devices for the magnetic exploration of fossils containing materials with a high magnetic permeability.

Prospects for the development of this area allow one to:

- bring geophysical services to the service market on a new scientific and technical production level;
- reduce the environmental burden on nature by replacing magnetometric measurements with energy-saving, environmentally safe technology;
- ensure the export potential of magnetometric equipment.

Author Contributions: Conceptualization, D.F.; Methodology, V.K.; Software, V.C.; Validation, V.K.; Formal Analysis, D.F., A.K. and V.C.; Investigation, V.K.; Resources, A.K.; Data Curation, A.M.; Writing—Original Draft Preparation, N.O. and D.N.; Writing—Review and Editing A.K. and D.F.; Project Administration Y.P. and D.N.; Funding Acquisition Y.P. All authors have read and agreed to the published version of the manuscript.

Funding: This research received no external funding.

Institutional Review Board Statement: Not applicable.

Informed Consent Statement: Not applicable.

Data Availability Statement: Not applicable.

Conflicts of Interest: The authors declare no conflict of interest.

References

1. Adelman, R.; Gumerov, N.A.; Duraiswami, R. FMM/GPU-Accelerated Boundary Element Method for Computational Magnetics and Electrostatics. *IEEE Trans. Magn.* **2017**, *53*, 1–11. [CrossRef]
2. Kim, D.H.; Park, I.H.; Park, M.C.; Lee, H.B. 3-D magnetostatic field calculation by a single layer boundary integral equation method using a difference field concept. *IEEE Trans. Magn.* **2000**, *36*, 3134–3136.
3. Andjeli´c, Z.; Ishibashi, K. Double-layer BEM for generic electrostatics. In Proceedings of the 2016 IEEE Conference on Electromagnetic Field Computation (CEFC), Miami, FL, USA, 1 November 2016.
4. Andjeli´c, Z.; Ishibashi, K.; Barba, P.D. Novel double-layer boundary element method for electrostatic analysis. *IEEE Trans. Dielectr. Electr. Insul.* **2018**, *25*, 2198–2205. [CrossRef]
5. Ishibashi, K.; Yoshioka, T.; Wakao, S.; Takahashi, Y.; Andjelic, Z.; Fujiwara, K. Improvement of unified boundary integral equation method in magnetostatic shielding analysis. *IEEE Trans. Magn.* **2014**, *50*, 105–108. [CrossRef]
6. Ishibashi, K.; Andjelic, Z.; Takahashi, Y.; Takamatsu, T.; Fukuzumi, T.; Wakao, S.; Fujiwara, K.; Ishihara, Y. Magnetic Field Evaluation at Vertex by Boundary Integral Equation Derived from Scalar Potential of Double Layer Charge. *IEEE Trans. Magn.* **2012**, *48*, 459–462. [CrossRef]
7. Ishibashi, K.; Andjelic, Z. Generalized magnetostatic analysis by boundary integral equation derived from scalar potential. *IEEE Trans. Magn.* **2013**, *49*, 1533–1536. [CrossRef]
8. Telegin, A.P.; Klevets, N.I. Calculation of an axisymmetric current coil field with the bounding contour integration method. *J. Magn. Magn. Mater.* **2004**, *277*, 257–262. [CrossRef]
9. Filippov, D.M.; Shuyskyy, A.A. Improving efficiency of the secondary sources method for modeling of the three-dimensional electromagnetic field. *Prog. Electromagn. Res. M* **2019**, *78*, 19–27.
10. Neethu, S.; Nikam, S.; Wankhede, A.K.; Pal, S.; Fernandes, B.G. High speed coreless axial flux permanent magnet motor with printed circuit board winding. In Proceedings of the IEEE Industry Applications Society Annual Meeting, Cincinnati, OH, USA, 1–8 October 2017.
11. Aydin, M.; Gulec, M. A new coreless axial flux interior permanent magnet synchronous motor with sinusoidal rotor segments. *IEEE Trans. Magn.* **2016**, *52*, 1–4. [CrossRef]
12. Price, G.P.; Batzel, T.D.; Comanescu, M.; Muller, B.A. Design and testing of a permanent magnet axial flux wind power generator. In Proceedings of the 2008 IAJC-IJME International Conference, Music City Sheraton, Nashville, TN, USA, 17–19 November 2008.
13. Andjelic, Z.; Ishibashi, K.; Lage, C.; Di Barba, P. On a Study of Magnetic Force Evaluation by Double-Layer Approach 2020. *IEEE Trans. Magn.* **2020**, *56*, 8956056. [CrossRef]
14. Ryu, K.; Yoshioka, T.; Wakao, S.; Ishibashi, K.; Fujiwara, K. Magnetostatic Shield Analysis by Double-Layer Charge Formulation Using Difference Field Concept. *IEEE Trans. Magn.* **2016**, *52*, 7205604. [CrossRef]
15. Ryu, K.; Wakao, S.; Takahashi, Y.; Ishibashi, K.; Fujiwara, K. A study on multiply connected domain processing methods in magnetostatic field analysis by boundary integral equations. *IEEE Trans. Power Energy* **2017**, *137*, 132–137. [CrossRef]
16. Filippov, D.M.; Berzhansky, V.N.; Shuyskyy, A.A.; Lugovskoy, N.V. Mathematical modeling and magneto-optical visualization of the electromagnetic field in the neighborhood of defects in conductive materials. *CEUR Workshop Proc.* **2021**, *2914*, 324–330.
17. Filippov, D.M.; Shuyskyy, A.A.; Kazak, A.N. Numerical and experimental analysis of an axial flux electric machine 2020 Proceedings-2020 International Conference on Industrial Engineering, Applications and Manufacturing. *ICIEAM* **2020**, 9112004. [CrossRef]
18. Ishibashi, K.; Andjelic, Z.; Takahashi, Y.; Fujiwara, K.; Ishihara, Y. Some treatments of fictitious volume charges in nonlinear magnetostatic analysis by BIE. *IEEE Trans. Magn.* **2012**, *48*, 463–466. [CrossRef]
19. Yu, H.; Yuan, J. Improved differential field integral equation method. *J. Tsinghua Univ.* **2008**, *48*, 1073–1076.
20. Hafla, W.; Buchau, A.; Rucker, W.M. Accuracy improvement in nonlinear magnetostatic field computations with integral equation methods and indirect total scalar potential formulations. *COMPEL-Int. J. Comput. Math. Electr. Electron. Eng.* **2006**, *25*, 565–571. [CrossRef]

21. Ishibashi, K.; Andjelic, Z.; Takahashi, Y.; Fujiwara, K.; Ishihara, Y. Magnetostatic analysis by BEM with magnetic double layer as unknown utilizing volume magnetic charge. *Int. J. Appl. Electromagn. Mech.* **2012**, *39*, 711–717. [CrossRef]
22. Charge Ishibashi, K.; Andjelic, Z. Nonlinear magnetostatic BEM formulation using one unknown double layer. *COMPEL-Int. J. Comput. Math. Electr. Electron. Eng.* **2011**, *30*, 1870–1884. [CrossRef]
23. Young, J.C.; Gedney, S.D. A locally corrected Nyström formulation for the magnetostatic volume integral equation. *IEEE Trans. Magn.* **2011**, *47*, 2163–2170. [CrossRef]
24. Young, J.C.; Gedney, S.D.; Adams, R.J. Quasi-mixed-order prism basis functions for nyström-based volume integral equations. *IEEE Trans. Magn.* **2012**, *48*, 2560–2566. [CrossRef]
25. Valve Wang, S.; Cheng, J.; Huang, K.; Zhu, J.; Zhang, W. Research on the Electromagnetic Characteristics of UHV-VSC Converter. In Proceedings of the 2020 7th IEEE International Conference on High Voltage Engineering and Application, ICHVE 2020-Proceedings, Beijing, China, 6–10 September 2020.
26. Wang, S.; Cheng, J.; Huang, K.; Zhao, L.; Lin, J. Electric field calculation of UHV-VSC valve hall based on instantaneous potential load method. *IET Conf. Publ.* **2020**, *775*, 2260–2264.
27. Yu, H.Y.; He, J.L.; Lee, J.B.; Chang, S.H.; Zou, J. Adaptive Galerkin approach of indirect boundary element method for calculating 3D magnetostatic field with local updating algorithm. In Proceedings of the 2006 12th Biennial IEEE Conference on Electromagnetic Field Computation, Miami, FL, USA, 30 April–2 May 2006.
28. Filippov, D.M.; Kozik, G.P.; Shuyskyy, A.A.; Kazak, A.N.; Samokhvalov, D.V. A New Algorithm for Numerical Simulation of the Stationary Magnetic Field of Magnetic Systems Based on the Double Layer Concept 2020. In Proceedings of the 2020 IEEE Conference of Russian Young Researchers in Electrical and Electronic Engineering, St. Petersburg and Moscow, Russia, 27–30 January 2020.
29. Noguchi, S.; Kim, S. Development of numerical simulation method for magnetic separation of magnetic particles. In Proceedings of the 2010 Digests of the 2010 14th Biennial IEEE Conference on Electromagnetic Field Computation, Chicago, IL, USA, 9–12 May 2010.
30. Banucu, R.; Albert, J.; Scheiblich, C.; Reinauer, V.; Rucker, W.M. Design and optimization of a device with contactless actuation for 4-axis machining 2010. In Proceedings of the 2010 14th Biennial IEEE Conference on Electromagnetic Field Computation, Chicago, IL, USA, 9–12 May 2010.
31. Hafla, W.; Buchau, A.; Rucker, W.M. Application of fast multipole method to Biot-Savart law computations. In Proceedings of the 6th International Conference on Computational Electromagnetics, Aachen, Germany, 4–6 January 2006.
32. Zheng, Q.; Zeng, H. Multipole theory analysis of 3D magnetostatic fields. *J. Electromagn. Waves Appl.* **2006**, *20*, 389–397. [CrossRef]